Proceedings of the 21st ICSMGE, Vienna, Austria, 14 – 19 June 2026. Pistrol, Adam & Schweiger (eds.)
Published by: ÖGG, Austrian Society for Geomechanics, Salzburg, Austria, ISBN 978-3-9503898-4-5
https://doi.org/10.53243/ICSMGE2026-2384

Simulation analysis for static compressive load test and rapid load test of steel pipe pile

Kiyoka Kono, Koji Watanabe
Department of Civil Engineering, Aichi Institute of Technology, Toyota, Japan. f24706ff@aitech.ac.jp

Shihchun Lin, Shuichi Kamei
Engineering Department, Jibanshikenjo Co., Ltd., Tokyo, Japan.

ABSTRACT: This study aims to simulate Rapid Load Test (RLT) using a Finite Element Model (FEM) to examine the mechanism behind RLT interpretation methods. Static Load Test (SLT) is highly reliable for evaluating vertical bearing characteristics but is associated with high costs and long construction time. In contrast, RLT offers advantages in terms of cost and efficiency. However, unlike SLT, RLT includes both static and dynamic resistance, which complicates the interpretation process. Several interpretation methods for RLT have been proposed in the past, addressing most test cases. However, issues such as the rate effect have been reported by RLT researchers. To address this, the aim of this study is to develop an FEM that simulates both SLT and RLT using data from full-scale tests conducted by Jibanshikenjo Co., Ltd. on the same open-end steel pipe pile (SPP) with an outer diameter of 318.5 mm. The FEM is used to analyze and compare SLT and RLT results. In addition, the study considers geomaterial parameters and rate effects, focusing on how these factors influence RLT results. This paper highlights the significance of rate effect in RLT and shows how it can alter the interpretation of test results. By simulating RLT in the FEM, this study contributes to a deeper understanding of RLT's behavior and enhances its reliability as an efficient alternative to SLT.

KEYWORDS: Elasto-plastic FEM, case study, static load test, rapid load test, steel pipe pile.

1 INTRODUCTION

The vertical bearing characteristics of piles are evaluated through load tests. Static load tests (SLT) are considered reliable for assessing vertical bearing characteristics because they simulate actual loading conditions. However, SLT requires a large-scale reaction device, resulting in high costs and long construction times. As an alternative, dynamic load tests are increasingly being used to estimate pile bearing characteristics more efficiently. Among dynamic load tests, rapid load tests (RLT) offer advantages in terms of cost and construction time, as they do not require a reaction device. However, RLT test data contains dynamic resistance components of the ground and inertial force effects (hereafter referred to as dynamic effects). These dynamic effects need to be removed in order to accurately assess the static vertical bearing characteristics.

Currently, the UnLoading Point Connection (ULPC) method is used in standard evaluations. However, an updated method - the UnLoading Point Connection method invoking Case method (ULPC_CM), which incorporates the Case method - is being considered in the revised standards, as described in Lin et al., 2023 (1). Since both methods include dynamic effects, a quantitative evaluation of these effects is essential. By clarifying the mechanism of dynamic effects, RLT results can be interpreted with greater accuracy, allowing for a more rational assessment of pile vertical bearing characteristics. In this study, full-scale vertical load tests were conducted, and the validity of the analytical method was examined by comparing RLT results using the ULPC and ULPC_CM methods. Additionally, a simulation analysis of SLT was performed to assess the validity of the modeling and parameter evaluation methods, with the aim of adapting them for RLT simulation analysis. Furthermore, triaxial compression tests at different loading rates were also conducted on sandy soil to verify the validity of parameter evaluations taking into account rate effects.

2 FULL-SCALE VERTICAL LOAD TESTS

2.1 *Test overview*

Table 1 shows the speciation of the test pile. Steel channels were wielded on the outer surface of steel pipe pile to protect the sensors and cables.

Figure 1 shows the results of soil investigations, and embedment of the instrumented test piles. In addition, Figure 2 illustrates the arrangement of SPT and test pile. Accelerometers were set at the only top level (L1). Displacement transducer was only used in SLT.

2.2 *Result of pile load test (Lin et al., 2023 (2))*

Full-scale load tests were carried out in Sashima test yard of Jibanshikenjo Co. Ltd., Japan. SLT were carried out first, followed by the RLT 8 days later.

The SLT was conducted using a multi-cycle method, where the load was gradually increased in increments of 80 kN, reaching a maximum load of 1040 kN.

The RLT was performed using the soft cushion weight drop method, employing a weight of 3.5 tons. A total of 8 blows were conducted, with the drop height gradually increased from 0.01 m to 0.83 m. The relative loading duration $T_r = t_L/(2L/c)$ (where t_L = loading time) of the RLT was set as 5, which is in accordance with the JGS standard.

Figure 3 shows the static load-displacement relations of each level from SLT and RLT using the ULPC_CM method.

Table 1. Specifications of test piles.

Item	Value	
	Original	with protection
Pile length, L (m)	11.8	
Embedment length, L_d (m)	11.0	
Outer diameter, D_o (mm)	318.5	
Inner diameter, D_i (mm)	305.3	
Wall thickness, t_w (mm)	6.6	
Cross-sectional area, A (m^2)	0.00651	0.00926
Young's modulus, E_s (GPa)	205	
Density, ρ (ton/m^3)	7.81	
Bar wave velocity, c (m/s)	5123	
Mass, m (ton)	0.610	0.819

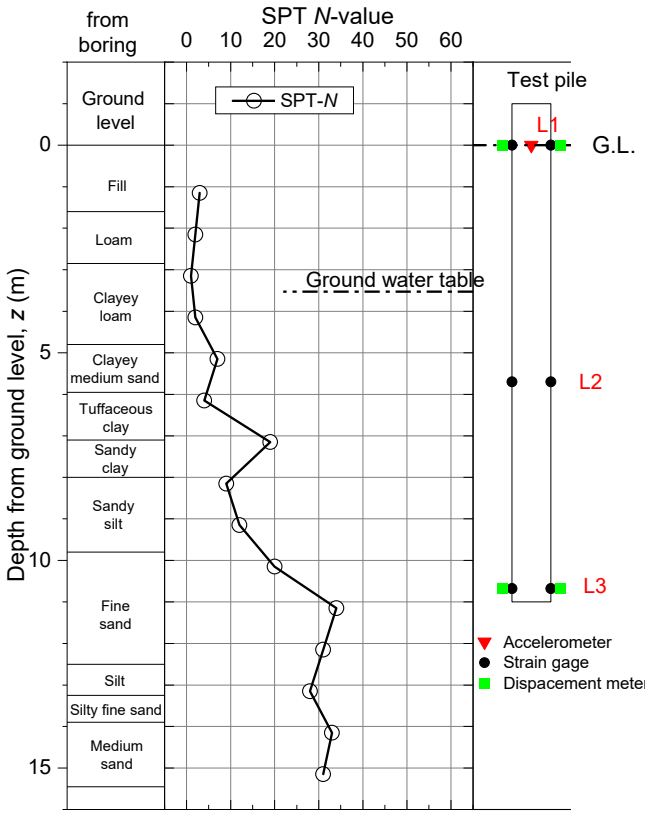

Figure 1. Profiles of soil layers, SPT *N*-values, to instrumented test pile.

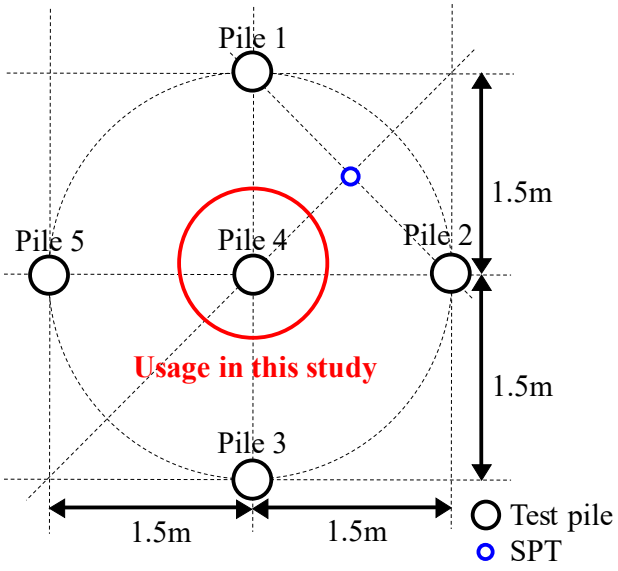

Figure 2. Arrangement of SPT and test pile.

3 SIMULATION ANALYSIS OF SLT

In this chapter, the validity of the modeling method and parameter evaluation was verified through a simulation analysis of the SLT results. The analytical model considered the symmetry of both the test pile and the surrounding ground, allowing for a 1/4 model representation of the analysis target. Figure 4 shows the analytical model and boundary conditions.

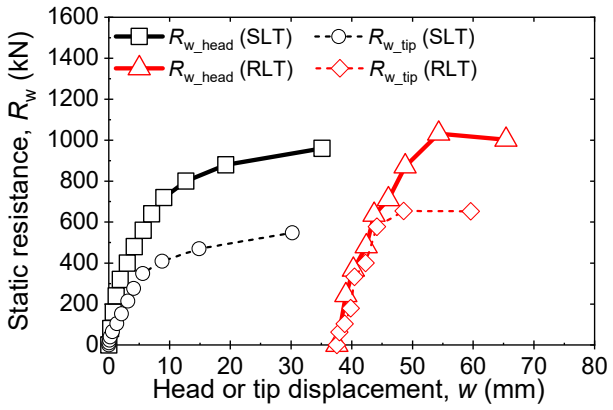

Figure 3. Profiles of soil layers, SPT *N*-values, to instrumented test pile.

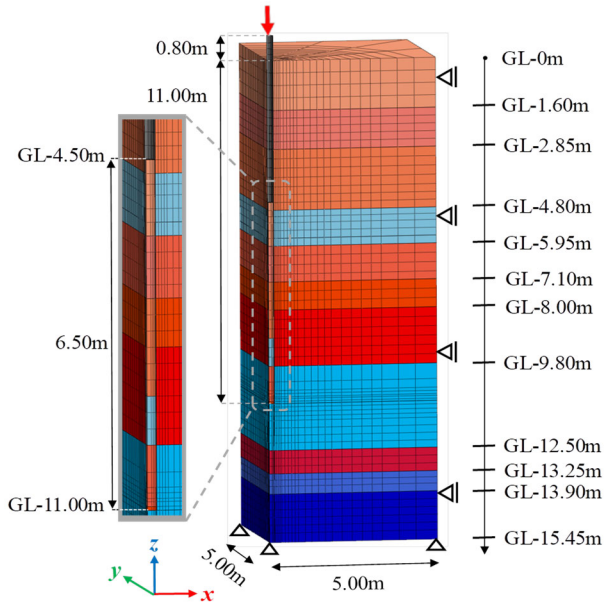

Figure 4. Profiles of soil layers, SPT *N*-values, to instrumented test pile.

The analysis was conducted as a step-by-step process, beginning with an initial stress analysis. Loads were then applied in 80 kN increments until the pile head reached a maximum of 960 kN.

Based on Kono et al., (2024) the deformation modulus E were calculated using the Specifications for Highway Bridges IV – Substructures (Road standard) as shown in Equation (1):

$$E = 2800N \quad (1)$$

Furthermore, for depths beyond the pile tip, the compaction effect during pile installation was considered, and the average value of the evaluation formulas from the Road standard and Uchida et al., (2019) was adopted, as equation (2) to (5):

$$V_s = 130N^{0.29} \text{ for clay} \quad (2)$$

$$V_s = 110N^{0.30} \text{ for sand} \quad (3)$$

$$G = V_s^2\rho \quad (4)$$

$$E = 2G(1+\nu) \quad (5)$$

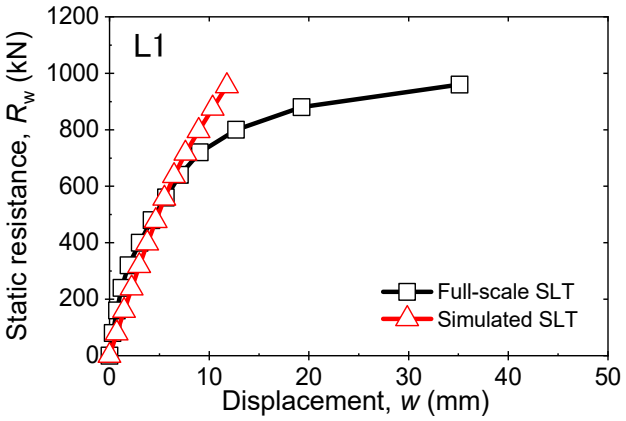

Figure 5. Comparison of static load-displacement relations between SLT and SLT simulation analysis (L1).

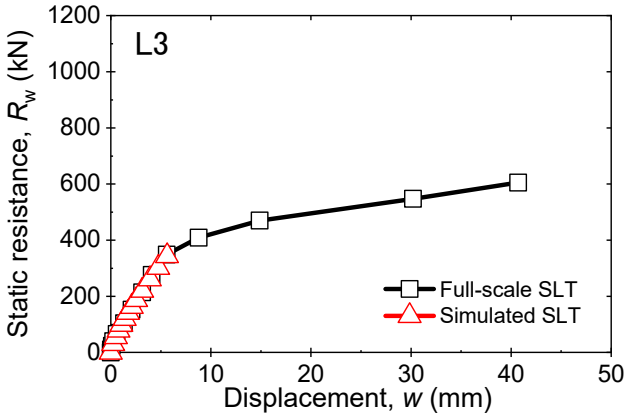

Figure 6. Comparison of static load-displacement relations between SLT and SLT simulation analysis (L3).

where, V_s = Shear wave velocity (m/s), G = Shear modulus (kPa), ρ = Density (g/cm^3), ν = Poisson's ratio (-)

Additionally, a 6.50 m soil plug, which was actually measured inside the steel pipe pile during construction, was modeled. Furthermore, a joint element was introduced at the boundary between the pile and the ground to simulate the shaft resistance characteristics. The joint element was approximated to a bilinear type based on the shaft resistance force-displacement relationship obtained from SLT, where the slope was set as the shear stiffness, and the maximum shaft resistance force was set as the adhesion strength.

Figure 5 and Figure 6 show the static load-displacement relation at each level. It was confirmed that the behavior from elastic region to the partial plastic region was reproduced. Based on this result, it is inferred that the modeling method and parameter evaluation used in this study are valid.

4 ELEMENT TEST

This chapter focuses on conducting triaxial compression tests with varying load rate on sandy soils to examine the rate effect of the geomaterial. The tests were conducted at constant strain rates ranging from 0.0005 cm/s to 25 cm/s, with confining pressures of either 100 kPa or 500 kPa. Based on the confinement pressures of sand layers in the analysis model - 55 kPa for the 4th layer, 81 kPa for the 8th layer, 102 kPa for the 10th layer, and 105 kPa for the 11th layer - the rate effect will be primarily analyzed using test results at 100 kPa.

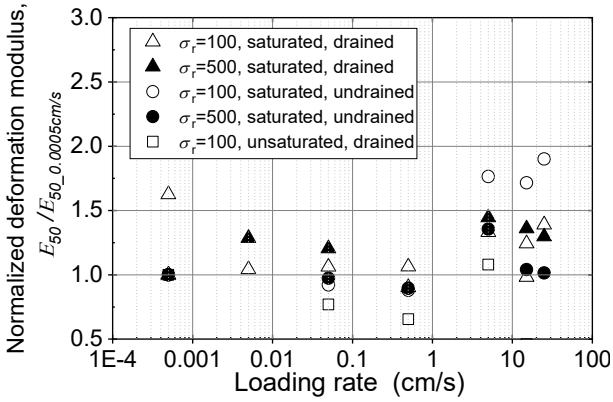

Figure 7. Relationships between normalized deformation modulus and loading rate.

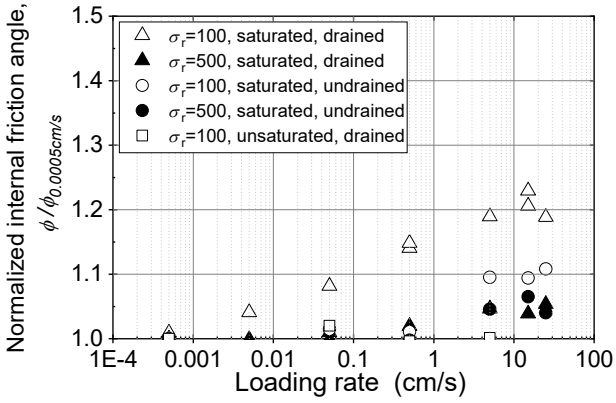

Figure 8. Relationships between normalized internal friction angle and loading rate.

The deformation modulus E_{50} obtained from each experiment was normalized using its value at the minimum loading rate. Likewise, the internal friction angle was normalized following the same method. The normalized deformation modulus-loading rate relationship is shown in Figure 7, while the normalized internal friction angle-loading rate relationship is presented in Figure 8.

Regarding the normalized deformation modulus-loading rate relationship in Figure 7, when the loading rate ranges from 0.0005 cm/s to 0.5 cm/s, the normalized deformation modulus remains constant above 1.0, confirming the influence of the rate effect. The normalized deformation modulus increases when the loading rate exceeds 0.5 cm/s, reaching about 1.5 at loading rates between 5 cm/s and 25 cm/s. In other words, the rate effect on the deformation modulus must be accounted for when the loading rate is either between 0.5 cm/s and 5 cm/s or exceeds 5 cm/s.

In Figure 8, the normalized internal friction angle-loading rate relationship, the influence of the rate effect was confirmed for loading rates between 0.0005 cm/s and 0.05 cm/s. The rate effect was found to be more significant at loading rates greater than 0.05 cm/s. For loading rates between 0.5 cm/s and 25 cm/s, the normalized internal friction angle was about 1.25, without a constant value. Therefore, the rate effect on both the deformation modulus and the internal friction angle must be considered.

The aforementioned rate effect is incorporated into the calculation of the speed at the tip of the hanger at each drop

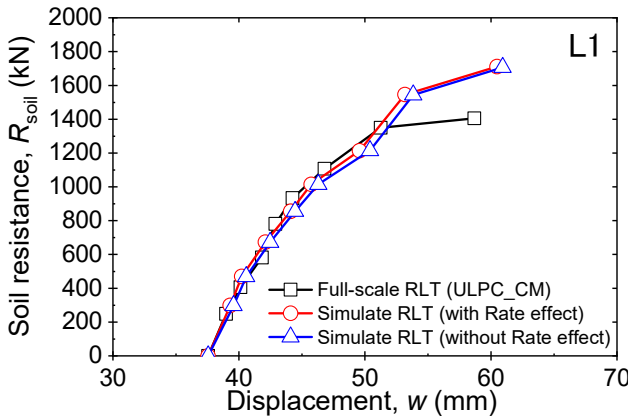

Figure 9. The skeleton curves at the maximum load for the load-displacement relationship at the pile head (L1).

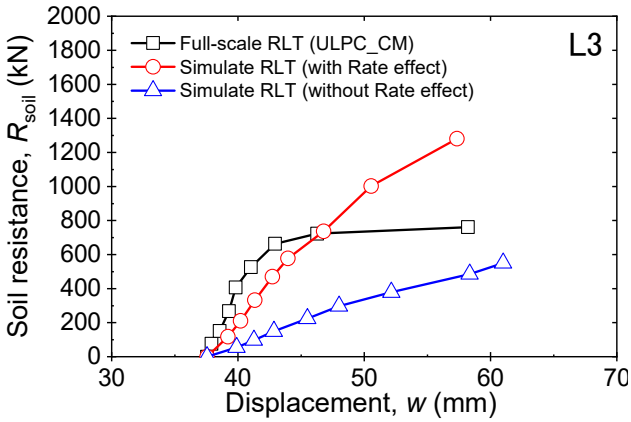

Figure 10. The skeleton curves at the maximum load for the load-displacement relationship at the pile tip (L3).

height of the heavy hammer in the RLT. The results showed that when the weight dropped from a height of 0.01 m, the deformation modulus was about 1.3 times larger, and the internal friction angle was about 1.25 times larger. When the weight dropped from a height of 0.03 m to 0.83 m, the deformation modulus was estimated to be about 1.4 times larger, and the internal friction angle was estimated to be about 1.25 times larger. In summary, the rate effect on the geomaterial parameters can be reflected in the RLT simulation analysis, with the expectation that it will enable more accurate results.

5 SIMULATION ANALYSIS OF RLT

In this chapter, we will discuss the modeling techniques used in SLT and the simulation analysis of RLT with respect to the field parameters. The analysis involves performing an initial stress analysis based on construction stage analysis and deadweight, followed by applying the load time history from full-scale RLT on the pile head at each drop height to calculate the dynamic load. In practice, based on the results presented in Section 4.2, we conducted a simulation analysis that takes into account the rate effect on the ground parameters in sandy soil.

Figure 9 shows the skeleton curves of the load-displacement relationship (the pile head) at the maximum load, both before and after considering the rate effect. The results indicate similar trends in both cases up until the final 2 blows. Both methods overestimated the R_{soil} starting from the second-to-last blow (drop height = 0.53 m).

Figure 10 shows the skeleton curves at the maximum load for the load-displacement relationship at the pile tip. It can be seen that the skeleton curve of the simulated RLT with the rate effect closely aligns with the initial part of the curve from the full-scale RLT. However, as in the previous case, the R_{soil} is overestimated starting from the second-to-last blow. In contrast, the curve without the rate effect is significantly lower than that of the full-scale RLT. These results confirm the presence of the rate effect at the pile tip.

6 CONCLUSION

This study conducted experiments on SLT and RLT, explained the analytical method and vertical bearing characteristics of SLT, verified the appropriateness of the modeling method and parametric evaluation, and applied SLT's simulation analysis to RLT. In this context, a comparison and examination will be performed by considering the reflection of the rate effect on the parameters.

(1) The analysis of SLT confirmed that both elastic behavior and partial plastic deformation across the entire cross-section could be reproduced. This suggests the validity of the modeling method and parametric evaluation, supporting its potential application in RLT simulation analysis.

(2) In the normalized deformation modulus-loading rate relationship, the rate effect was observed in the range of 0.0005 cm/s to 0.5 cm/s and again at speeds exceeding 5 cm/s. In the normalized internal friction angle-loading rate relationship, the rate effect was confirmed for loading rates between 0.0005 cm/s and 0.05 cm/s, with a more pronounced effect at speeds above 0.5 cm/s.

(3) The results of the simulated RLT with the rate effect show similar trends at low drop heights and overestimate the R_{soil} at both the pile head and tip. However, the results without the rate effect show similar behavior at the pile head, while the pile tip is underestimated. It can be concluded that the rate effect must be considered when conducting RLT simulations. These findings underscore the importance of appropriately evaluating parameters when considering the rate effect in RLT analysis.

7 REFERENCES

Lin, S., Kamei, S., Yamamoto, I., and Matsumoto, T. 2023. Hybridnamic rapid load testing with UnLoading Point Connection method invoking Case method. *Proc. on 17th Int. Conf. on Asian Regional Conference on Soil Mechanics and Geotechnical Engineering*, Astana.

Lin, S., Watanabe, K., Kamei, S., Yamamoto, I., and Matsumoto, T. 2023. Comparative static and rapid load tests on steel pipe piles: A case study at Sashima test yard. *Proc. on 5th Int. Conf. on Geotechnics for Sustainable Infrastructure Development*, Hanoi.

Japanese Geotechnical Society (JGS) 2002. JGS 1815-2002 Method for Rapid Load Test of Single Piles.

Kono, K., Lin, S., Kamei, S., and Watanabe, K. 2024. Simulation analysis for static compressive load test of steel pipe piles. *Proc. on 14th Int. Conf. on GEOMATE 2024*, Pattaya.

Japan Road Association 2017. Specification for Highway Bridges: Part IV Substructures.

Uchida, A., Tokimatsu, K., and Tsujimoto, K. 2019. A study on estimation of S-wave velocity by *N*-value, *Technical Report of the Architectural Institute of Japan*, Japan, 119-122. (in Japanese)